Comparison of Flow and Cavitation Processes in Conventional and Group-Hole Diesel Injector Nozzles using Numerical Simulations

W. G. Lee* and R. D. Reitz
Engine Research Center
University of Wisconsin-Madison
Madison, WI 53706 USA

Abstract

The high speed, transient cavitating flow distribution inside diesel injector nozzles with consideration of the opening and closing needle valve is calculated using a generalized equation of state (EOS) to describe the fluid density, a homogeneous equilibrium model (HEM) for phase change, and an arbitrary moving mesh to account for needle motion. The KIVA-3V code was modified for the generalized equation of state, and an isothermal acoustic speed formulation, related to the void fraction in two phase flow, was used to account for the rate of fluid volume change due to pressure changes (dV/dP). The needle valve motion was implemented by exploiting the piston motion feature already available in the KIVA code, using the arbitrary Lagrangian-Eulerian (ALE) approach. Cavitation zone formation and development were simulated and compared in three-dimensional real-sized nozzle models for both conventional multi-hole and group-hole arrangements. The effects of geometric factors of the group-hole nozzle on the discharge coefficient, area contraction and density variation were investigated. The temporal evolution of cavitation during the opening and closing of the needle valve was also studied. It is shown that pressure waves and transient flow effects brought about by the time-varying needle motion significantly affect the flow structure and cavitation processes.

Introduction

The combination of higher injection pressure and smaller diameter nozzles has been useful to reduce PM and NOx emissions from diesel engines. However, it has been reported that smaller diameter nozzles can entrain too much air and give a shorter spray penetration, resulting in increased PM, especially under high-speed and high-load conditions [1]. To overcome this drawback, the concept of using group-hole nozzles has been proposed [2]. The idea is to arrange small-sized holes closely spaced so as to reduce spray droplet size while restricting air entrainment and maintaining the penetration length. Even though the merit of the group-hole nozzle in a real combustion engine is still under debate [3], there has been much research on the structure of the sprays from various configurations of group-hole nozzles [4, 5, 6]. Recently Park et al. [7] numerically investigated the effect of group-hole nozzle layout on diesel engine combustion and emissions. In their research the injection conditions of the two sprays from a group-hole injector were assumed to be identical. However, different flow structures may yield different rates of injection and cavitation inside the two holes in a group-hole injector due to the different layouts of the nozzle holes.

Since the discharge coefficient of a nozzle orifice depends highly on the injector design and is not constant during the injection process, it is important to establish a method to predict the transient rate of injection. Many attempts have been made, including visualization and simulation studies. However, transient cavitation inside the injector nozzle passage increases the uncertainty in measurements and leads to difficulty in modeling. Several approaches have been proposed to simulate highly transient, cavitating flow. One of them is the single-fluid approach also used in the present study. Based on the Homogeneous Equilibrium Model of Wallis [8], the method treats the two-phase mixture as one compressible fluid. HEM was applied to simulate cavitation phenomena in 2-dimensional nozzle passage geometries by Schmidt et al. [9]. The HEM method was then successfully implemented into the KIVA code and was further developed as a code called CAVIF [10]. In their model [9,10], the pressure was calculated directly from the equation of state of the mixture, and the flow was treated as laminar. Ning et al. [11] applied the HEM method in conjunction with the Eulerian-Lagrangian Spray Atomization model [12]. They proposed a new pressure equation that was derived from the continuity equation, and some modifications to the turbulence models were also proposed.

*Corresponding author

There are many other cavitation models, such as the three-fluid approach of Grogger et al. [13] and the cavitation bubble-tracking model of Gavaises et al. [14]. However, a single-fluid model is relatively easy to implement into existing codes and with some modifications, it can be combined with turbulence and spray models. Recently, Lee et al. [15] implemented the HEM approach and the generalized equation of state into the KIVA code and investigated phenomena occurring during the end-of-injection event. This method was also used in the present study to investigate the structure of the flow and cavitation inside both conventional multi-hole and group-hole injectors.

Numerical Methods

In this study, the two-phase flow was assumed to be one homogeneous mixture of vapor and liquid, as with the Homogeneous Equilibrium Model. The barotropic equation of state of Wallis [8] was used. Under the assumption of constant temperature, the acoustic speed of the two-phase flow is expressed as:

$$\frac{1}{a^2} = \left[\alpha\rho_v + (1-\alpha)\rho_l\right]\left[\frac{\alpha}{\rho_v a_v^{\,2}} + \frac{1-\alpha}{\rho_l a_l^{\,2}}\right] \tag{1}$$

where α is the void fraction, defined as:

$$\alpha = \frac{\rho_l - \rho}{\rho_l - \rho_v} \tag{2}$$

To derive the equation of state, the pressure was integrated directly from the equation:

$$dP = a^2 d\rho \tag{3}$$

resulting in [9]:

$$P = \rho a_v^{\,2} \qquad if\ \rho \le \rho_v \tag{4}$$

$$P = P_l^{sat} + P_{vl}\log\left[\frac{\rho_v a_v^{\,2}(\rho_l + \alpha(\rho_v - \rho_l))}{\rho_l\left(\rho_v a_v^{\,2} - \alpha\left(\rho_v a_v^{\,2} - \rho_l a_l^{\,2}\right)\right)}\right] \qquad if\ \rho_v < \rho < \rho_l \tag{5}$$

$$P = P_l^{sat} + (\rho - \rho_l)a_l^{\,2} \qquad if\ \rho \ge \rho_l \tag{6}$$

where

$$P_{vl} = \frac{\rho_v a_v^{\,2}\rho_l a_l^{\,2}(\rho_v - \rho_l)}{\rho_v^{\,2} a_v^{\,2} - \rho_l^{\,2} a_l^{\,2}} \tag{7}$$

$$P_l^{sat} = P_v^{sat} + P_{vl}\log\left[\frac{\rho_v^{\,2} a_v^{\,2}}{\rho_l^{\,2} a_l^{\,2}}\right] \tag{8}$$

In this study a modified code based on the KIVA-3V Release 2 code [16] was used. Since the standard KIVA code uses the ideal gas assumption for the equation of state, a generalized implementation of the equation of state was needed. The method introduced by Trujillo et al. [17] was adopted:

$$V^C = V^P + \left.\frac{\partial V^P}{\partial P}\right|_S \left(P^C - P^P\right) \tag{9}$$

$$\left.\frac{\partial V^P}{\partial P}\right|_S = -\frac{M}{\rho^2}\left.\frac{\partial \rho^P}{\partial P}\right|_S = -\frac{V}{\rho}\left.\frac{\partial \rho^P}{\partial P}\right|_S = -\frac{V}{\rho}\frac{1}{a_S^{\,2}} \tag{10}$$

where a_s is the isentropic speed of sound.

Trujillo et al. [17] showed an application of the Peng-Robinson equation with this method. Recently, Lee et al [15] implemented the above equations of state (4)~(8) into the KIVA code using the generalized forms of Eqs. (9) and (10), and showed various simulations of cavitating flows inside injector nozzles. The same approach was also used in this study. A detailed description of the methods and the physical properties of the injected diesel fuel can be seen in [15].

Computational meshes were generated for a multi-hole nozzle and for three group-hole nozzles. Since the nozzles have 8 single holes or 8 groups of 2 holes in the circumferential direction, the meshes were modeled as 1/8 sector meshes with periodic boundaries. The shapes of the computational domains are shown in Figure 1, and the important dimensions are shown in Table 1. The exit pressure P_2 was set as 5 bar, and the pressure difference ΔP between the inlet and exit was set as 1500 bar. The computational domains consists of 3 regions. The first is for a sac volume and the gap between the needle and the housing, the second is for the high pressure zone, and the third is for the nozzle passage and orifice. When the needle is moving, the mesh in region 1 is added to or removed by the snap-

ping algorithm in the KIVA code. The location of the needle is defined in Figure 2. At the start of the simulation, the pressure in regions 1 and 3 was 5 bar, and the pressure in region 2 was 1505 bar.

Results and Discussion

The flows and cavitation phenomena inside the injectors were simulated for the 4 different nozzle geometries. In Figure 3, the transient mass fluxes due to needle movement are shown as discharge coefficients (C_d) defined by:

$$C_d = \frac{\int \rho u \, dA}{\rho_f U_b A} \tag{11}$$

where U_b ($= \sqrt{2\Delta P / \rho_f}$) is the Bernoulli velocity and ρ_f is the nominal density of the fuel at 5 bar.

Cavitation development during the needle valve opening event is shown in Figure 4. For all cases, the discharge coefficients already reached about 90 % of their maximum values when the needle valves were opened to 0.1 mm. The maximum C_d was about 0.6 for the Single Hole Nozzle (SHN). For the Group Hole Nozzle #1 (GHN1), the flow rate passing the lower nozzle hole was decreased, mainly because the lower nozzle is attached to the sac volume at an oblique angle of about 41 degrees. This leads to flow separation at the nozzle entrance and causes cavitation to occur at the entrance of the lower hole, as shown in Figure 4.

If the lower nozzle hole is exactly perpendicular to the nozzle sac surface, as in GHN3, then the C_d of the lower nozzle passage is seen to increase, and is even slightly larger than that of the upper nozzle. However, this kind of arrangement could induce more entrainment of the surrounding air and acts as 16 holes with different targeting points, which is not consistent with the concept of group-hole nozzles. Cavitation in this nozzle developed mainly in the lower hole, because the flow direction turns suddenly after following the sac volume surface.

The other way to balance the mass fluxes of both holes may be to locate the two holes closer, like GHN2. In this case the lower nozzle is nearly perpendicular to the sac volume surface and the arrangement respects the concept of the group-hole nozzle, that favors production of small SMD and air entrainment equivalent to the single hole nozzle. However, with the closer hole arrangement, the C_d's of both nozzles were found to be smaller than that of the SHN, despite the fact that the flow rates are well balanced. If the two holes are located too close together, the mass fluxes between the two holes has to be divided, and the flux at the upper side of the lower hole is not sufficient. In addition, the flows entering neighboring holes interact with each other, and this make the C_d's fluctuate, as can be seen in Figure 3. When the lower side of the entrance of the upper hole attracts more mass flux, the upper side of the entrance of the lower hole suffers from a lack of entering flux, which leads to a rotating flow and resulting cavitation, as shown in Figure 4. Therefore, a desirable arrangement of the group-hole nozzle may be to arrange sufficiently separated holes, which are both normal to the wall. A possible way to achieve this is a group-hole nozzle on a cone shaped sac volume, not a hemispherical one.

When the needle valve closes, cavitation is augmented inside the nozzle passages, as shown in Figure 5. Cavitation increases because the pressure drops inside the nozzle passage as the entering mass flux at the passage entrance is rapidly decreased by blocking by the needle while the exit mass flux is decreased relatively slowly due to inertia. Thus, the flow is stretched and its pressure drops. However, if the needle closing speed is not fast enough, this phenomenon may not happen [15]. At the end of the needle closing event, the increased cavitation reaches the exit of the nozzle and outward mass flux is maintained positive for a period of about 0.025 ms after the needle is fully closed at t=0.625 ms.

It is interesting to note that the cavitation location changed direction in the SHN, GHN1 and GHN3 nozzles during the injection due to the change of flow direction. When the needle lift is high, the mass flux is supplied uniformly (SHN) or mainly upward (GHN1, GHN3). However, when the lift is low, the flow passing through the small gap between the needle and housing is injected toward the center of the sac volume and then turns back upward to the holes. These flow details change the cavitation inception point in the upper nozzle holes, as shown in Figure 6, and in the streamline patterns.

The transient behaviors of velocity and density are shown in Figure 7. The velocity and density were averaged over the exit area and normalized by the Bernoulli velocity U_b and the nominal density ρ_f, respectively. A value of density ratio (ρ/ρ_f) less than unity means that vapor generated by cavitation reaches the exit. In the SHN case, the cavitation vapor reached the exit intermittently and filled almost 40 % of the exit area when the needle valve closes. On the other hand, in the GHN1 case, the cavitation vapor did not reach the exit in most of the injection period, except in the late period of the needle valve closing event at the upper hole. The velocity ratio U_{mean}/U_b is the same as C_d when ρ/ρ_f is unity, but it is larger than C_d when cavitation reaches the exit. For example, in the SHN case, at the

time when the valve is fully closed (t=0.625 ms), U_{mean}/U_b remains as high as 0.1 if cavitation is augmented, whereas the C_d drops to 0.05.

Figure 8 shows the velocity distribution at the exit of the injector nozzles at t=0.342 ms, which represents the steady state injection period at the time just before the needle closing event. The velocity distribution at the exit of the SHN is more uniform than those of the upper holes the GHNs, even though the nozzles are attached at the same position to the sac volumes. The velocity distribution at the exit of the upper holes of GHN1 and GHN3 are nearly same, but it is different at the upper hole of the GHN2, due to the interaction with the lower hole. Obviously there is much discrepancy between the velocity distributions of the upper holes and those of the lower holes. The discrepancy undoubtedly influences the atomization process and should be reflected in next-generation spray models.

Conclusions

In this study, it has been shown that the current single-phased, HEM approach can be applied to investigate cavitation processes inside injector nozzles. Differences in the rate-of-injection for each hole can be predicted, as well as the detailed velocity distribution and vapor fraction at the nozzle exit. The results show that pressure waves and transient flow effects can lead to flow oscillation between closely spaced flow passages that can promote cavitation and presumably atomization of the resulting spray also. The present modeling method can be utilized to optimize nozzle shapes and hole arrangements to prevent or encourage cavitation. The results can be also used as an input condition for spray model improvement.

Nomenclature

		Subscripts		Superscripts	
a	speed of sound	v	vapor	C	corrected
P	pressure	s	isentropic	P	predicted
V	Lagrangian volume of a cell	l	liquid	sat	saturated
α	void fraction of mixture				
ρ	density				

Acknowledgement

The authors thank Cummins Engine Company for supporting this work.

References

1. Bergstrand, P. and Denbrantt, I., SAE 2001-01-2010, 2001.
2. Zhang, Y., Nishida, K., Nomura, S. and Ito, K., SAE 2003-01-3115, 2003.
3. Dohle, U., Krüger, M., Naber, D., Stein, J. O. and Gauthier, Y., *27th Vienna Motor Symposium*, April 2006.
4. Tokuda, H., Itoh, S., Kinugawa, M. and Shirabe, N. *26th Vienna Motor Symposium*, April 2005.
5. Nishida, K., Nomura, S., and Matsumoto, Y., *ICLASS 2006*, Paper No. ICLASS06-171, 2006.
6. Pawlowski, A., Kneer, R., Lippert, A. M. and Parrish, S. E., SAE 2008-01-0928, 2008.
7. Park, S. W. and Reitz, R. D., *ASME J. Eng. Gas Turbines and Power* 130: 032805 (2008)
8. Wallis, G. B., *One-dimensional two-phase flow*, McGraw-Hill, 1969.
9. Schmidt, D. P., Rutland, C. J. and Corradini, M. L., *Trans. SAE*, 106(3), pp. 1664-1673, (1997)
10. Habchi, C., Dumont, N. and Simonin, O., *Atomization and Sprays*, vol. 18, pp. 129–162, (2008)
11. Ning, W., Reitz, R.D., Diwakar, R., Lippert, A.M., SAE 2008-01-0936, 2008.
12. Blokkeel, G., Barbeau B. and Borghi, R., SAE 2003-01-0005, 2003.
13. Grogger, H. and Alajbegovic, A., *ASME Fluids Engineering Division Summer Meeting*, June 21-25, 1998.
14. Gavaises, M., Papoulias, D., Andriotis, A., Giannadakis, E., and Theodorakakos, A., SAE 2007-01-0246, 2007.
15. Lee, W. G. and Reitz, R. D., *ASME Internal Combustion Engine 2009*, May 2009.
16. Amsden, A.A., "KIVA-3V, Release 2, Improvements to Kiva-3V," LA-UR-99-915, Los Alamos, NM, 1999.
17. Trujillo, M.F., Torres, D.J. and O'Rourke, P.J., *International Journal of Engine Research*, Vol.5, No.3, (2004)

Table 1. Important dimensions of the injectors

Nozzle type	SHN	GHN1	GHN2	GHN3
# nozzle holes in a 1/8 sector	1	2	2	2
Hole diameter (mm)	0.127	0.09	0.09	0.09
Distance between hole axes (mm)	-	0.3	0.15	0.3 ~ 0.95
Included angle of hole A (deg)	165	165	165	165
Included angle of hole B (deg)	-	165	165	104

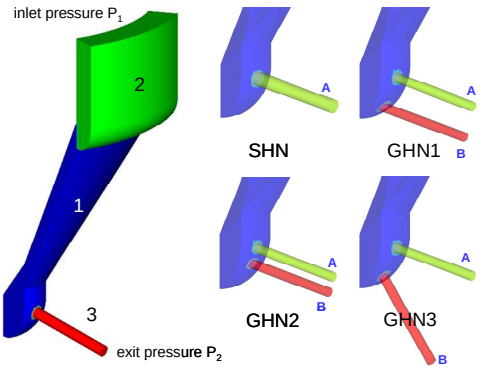

Figure 1. Computational geometries considered in the present study

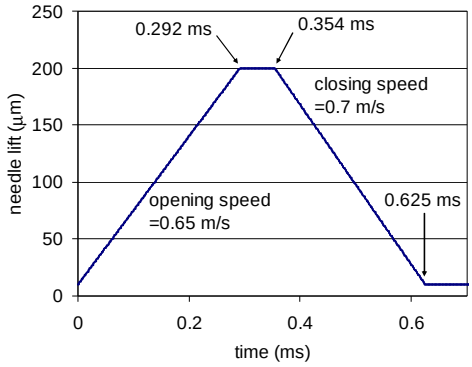

Figure 2. Needle lift motion

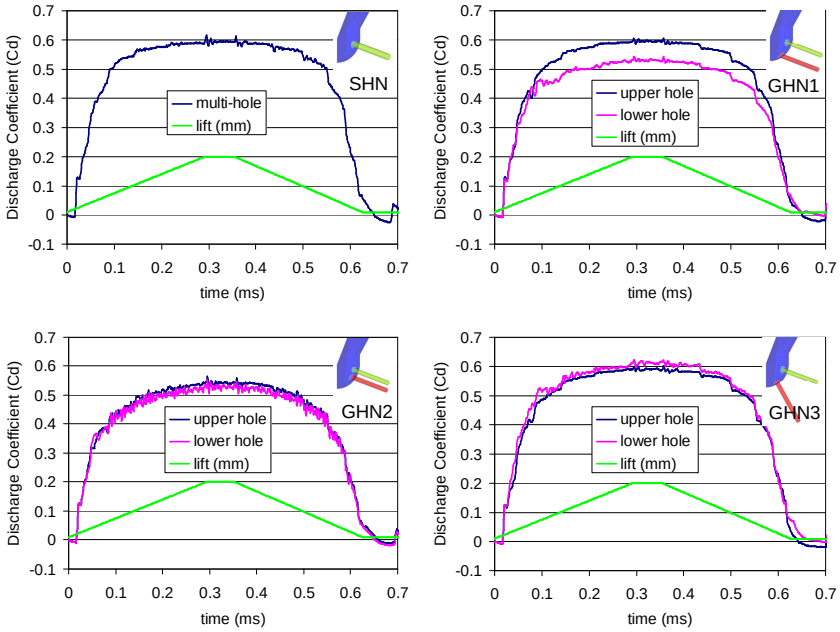

Figure 3. Discharge coefficients during injection processes in various injectors.

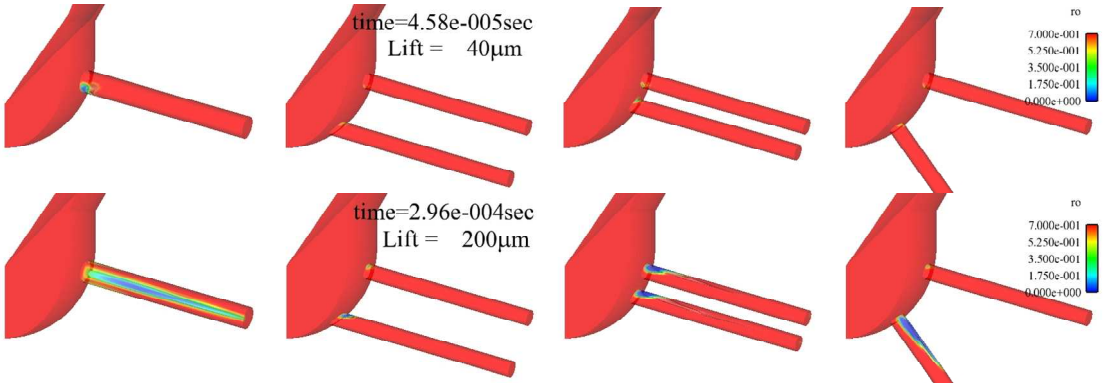

Figure 4. Cavitation development during nozzle opening event.

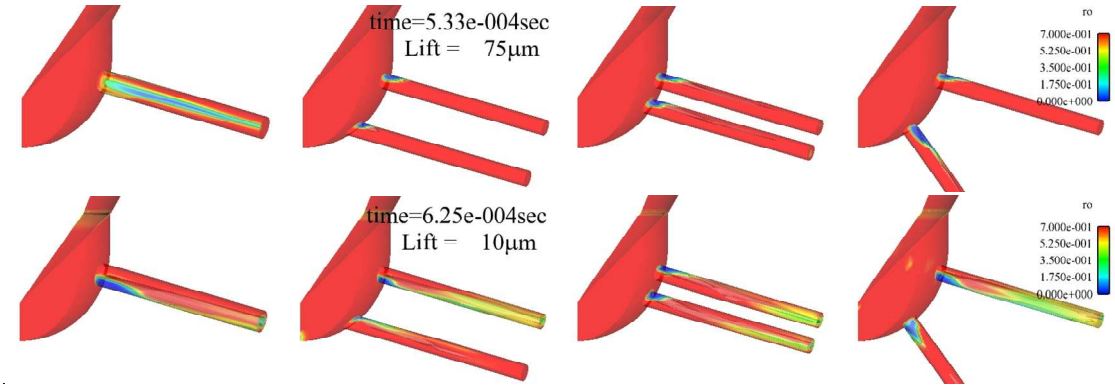

Figure 5. Cavitation augmentation during nozzle closing event.

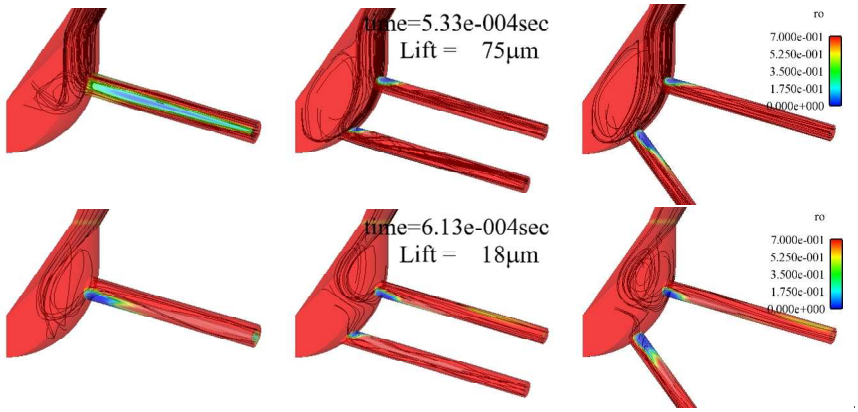

Figure 6. Change in streamline patterns during the nozzle closing event

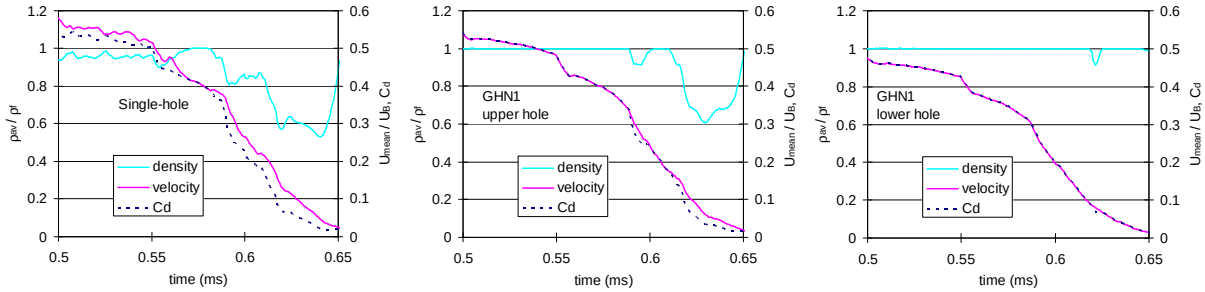

Figure 7. Transient changes in density and velocity during needle closing events

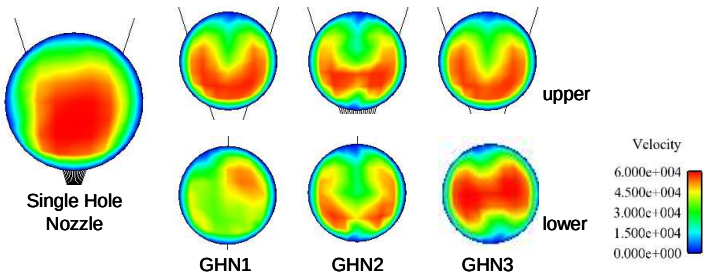

Figure 8. Example of exit velocity distributions at t=0.342 ms